SMC-TR-98-06

AEROSPACE REPORT NO.
TR-94(4935)-14

Fiber-Matrix Interphase Development in Carbon/Carbon Composites

15 January 1998

Prepared by

G. S. RELLICK, R. J. ZALDIVAR, and P. M. ADAMS
Mechanics and Materials Technology Center
Technology Operations

DTIC QUALITY INSPECTED 4

Prepared for

SPACE AND MISSILE SYSTEMS CENTER
AIR FORCE MATERIEL COMMAND
2430 E. El Segundo Boulevard
Los Angeles Air Force Base, CA 90245

Engineering and Technology Group

19980415 143

THE AEROSPACE
CORPORATION
El Segundo, California

MAJ. J. W. COLE
SMC/AXES

REPORT DOCUMENTATION PAGE

Public reporting burden for this collection of information is estimated to average 1 hour per response, including the time for reviewing instructions, searching existing data sources, gathering and maintaining the data needed, and completing and reviewing the collection of information. Send comments regarding this burden estimate or any other aspect of this collection of information, including suggestions for reducing this burden to Washington Headquarters Services, Directorate for Information Operations and Reports, 1215 Jefferson Davis Highway, Suite 1204, Arlington, VA 22202-4302, and to the Office of Management and Budget, Paperwork Reduction Project (0704-0188), Washington, DC 20503.

1. AGENCY USE ONLY (Leave blank)	2. REPORT DATE 15 January 1997	3. REPORT TYPE AND DATES COVERED

4. TITLE AND SUBTITLE
Fiber-Matrix Interphase Development in Carbon/Carbon Composites

5. FUNDING NUMBERS
F04701-93-C-0094

6. AUTHOR(S)
G. S. Rellick, R. J. Zaldivar, and P. M. Adams

7. PERFORMING ORGANIZATION NAME(S) AND ADDRESS(ES)

The Aerospace Corporation
Technology Operations
El Segundo, CA 90245

8. PERFORMING ORGANIZATION REPORT NUMBER

TR-94(4935)-14

9. SPONSORING/MONITORING AGENCY NAME(S) AND ADDRESS(ES)

Space and Missile Systems Center
Air Force Materiel Command
2430 E. El Segundo Blvd.
Los Angeles Air Force Base, CA 90245

10. SPONSORING/MONITORING AGENCY REPORT NUMBER

SMC-TR-98-06

11. SUPPLEMENTARY NOTES

12a. DISTRIBUTION/AVAILABILITY STATEMENT
Approved for public release; distribution unlimited

12b. DISTRIBUTION CODE

13. ABSTRACT (Maximum 200 words)

In carbon/carbon (C/C) composites—i.e., a composite in which a carbon matrix is reinforced with carbon fiber—when the matrix is derived from a thermosetting resin, we always observe a distinct, highly graphitizable, and well-oriented matrix interphase structure adjacent to the fibers. Qualitatively, the orientation of the interphase is the same as the fiber. It is important to note that thermosetting resins are nongraphitizing when heated in bulk; they form isotropic, amorphous "glassy" carbon. The structure of this interphase becomes more prominent, i.e., more graphitic, as the heat treatment exceeds about 2200°C. We have postulated elsewhere that the basis for this graphite interphase development is molecular orientation induced in the degradation of the polymer matrix to carbon as a consequence of restraint of pyrolysis shrinkage at the fiber-matrix interface. More specifically, we have hypothesized that the critical factor for development of lamellar graphite (by subsequent high-temperature heat treatment) in this interphase, rather than amorphous glassy carbon, is a state of multiaxial tensile deformation during pyrolysis. We have studied the structural details of the interphase region in more detail using transmission electron microscopy in conjunction with selected area (electron) diffraction (SAD). We have also examined the influence of matrix microstructure on fracture behavior by using an in-situ SEM flexure stage that allowed us to follow the crack tip as it advanced through the different microstructural regions.

The development of a graphitized-carbon interphase can have major effects on properties. Two are discussed in this publication. The first is the effect on matrix density and associated matrix shrinkage. The other is the effect on mechanical properties. The latter is much more complicated and involves phenomena such as crack-tip blunting in the interphase in the early stages of its development and longer-range crack deflection as well as intramatrix cohesive failure in the later stages of development (heat-treatment temperatures of 2400 and 2750°C) where the interphase becomes highly graphitized.

14. SUBJECT TERMS
Composites, Carbon-carbon, Carbon fibers

15. NUMBER OF PAGES
12

16. PRICE CODE

17. SECURITY CLASSIFICATION OF REPORT UNCLASSIFIED	18. SECURITY CLASSIFICATION OF THIS PAGE UNCLASSIFIED	19. SECURITY CLASSIFICATION OF ABSTRACT UNCLASSIFIED	20. LIMITATION OF ABSTRACT

Contents

Figures

INTRODUCTION

In carbon/carbon (C/C) composites—i.e., a composite in which a carbon matrix is reinforced with carbon fiber—it is found that when the matrix is derived from a thermosetting resin, we always observe a distinct, highly graphitizable and well-oriented matrix interphase structure adjacent to the fibers.[1,2] Qualitatively, the orientation of the interphase is the same as the fiber. It is important to note that thermosetting resins are nongraphitizing when heated in bulk; they form isotropic, amorphous "glassy" carbon. The structure of this interphase becomes more prominent, i.e., more graphitic, as the heat treatment exceeds about 2200°C. We have postulated[2] that the basis for this graphite interphase development is molecular orientation induced in the degradation of the polymer matrix to carbon as a consequence of restraint of pyrolysis shrinkage at the fiber-matrix interface. More specifically, we have hypothesized that the critical factor for development of lamellar graphite (by subsequent high-temperature heat treatment) in this interphase, rather than amorphous glassy carbon, is a state of multiaxial tensile deformation during pyrolysis.[2]

An example of this interphase structure is shown in Figure 1. The matrix is derived from polyarylacetylene (PAA) resin.[3,4] The fiber is the Amoco PX-7, open-wedge type. The photograph is from a scanning electron microscope (SEM), in which the specimen has been argon-ion etched following polishing. This ion-etching procedure has the effect of revealing the graphite layer-plane microstructure, particularly when the graphite layer planes are predominantly perpendicular to the plane of section. Using this approach, we can effectively distinguish the graphitic interphase zone from the matrix proper—i.e., that portion of matrix removed some distance from the fiber and which is not transformed to graphite. Figure 2 shows a longitudinal section of a PAA-based composite heat
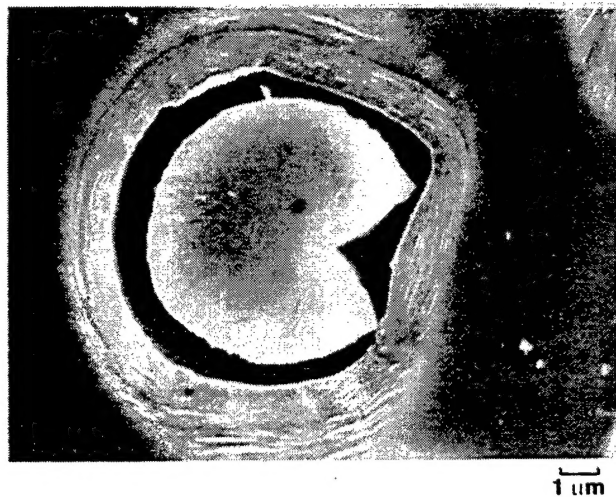

1 um

Figure 1. SEM showing "stress-graphitized" matrix around Amoco pitch-based PX-7 fiber following 2750°C HTT. Resin precursor was PAA. (Reprinted from *Carbon*, 29, R. J. Zaldivar and G. S. Rellick, "Some Observations on Stress Graphitization in Carbon-Carbon Composites," 1155–1163, Copyright 1991, with permission from Elsevier Sciences Ltd., Pergamon Imprint.)
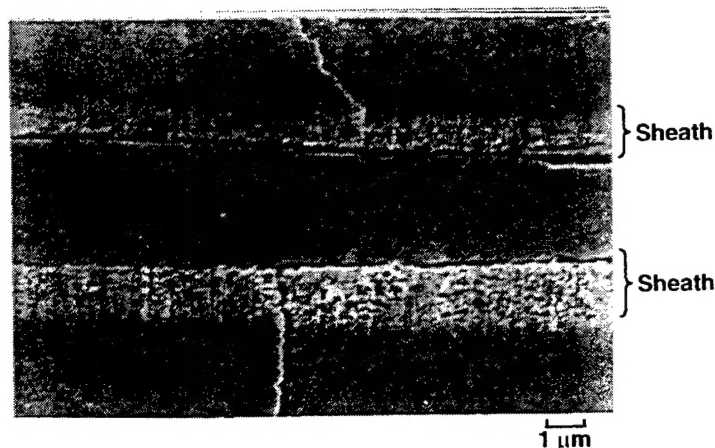
Figure 2. Longitudinal fiber-matrix interface of PAA/T50 composite heat treated to 2750°C, showing two strength-enhancing mechanisms: crack deflection along fiber-matrix interface (bottom), and blunting of crack tip within well-ordered sheath (top). (From "Processing Effects on the Mechanical Behavior of PAA-Derived C/C Composites," R. J. Zaldivar, G. S. Rellick, and J. M. Yang, *SAMPE J*. Reprinted by permission of the Society for the Advancement of Material and Process Engineering.)

treated to 2750°C that was strained to failure in tension; the fiber is the PAN-based T50 from Amoco. What we see in this very interesting photograph is both crack blunting and deflection in the interphase zone. The crack at the top of the photo is blunted at the interphase/glassy-carbon interface, whereas the bottom crack is deflected along the fiber/interphase boundary.

Our objective is to study the structural details of the interphase region in more detail using transmission electron microscopy in conjunction with selected area (electron) diffraction (SAD). We also wish to explore the influence of matrix microstructure on fracture behavior by using an in-situ SEM flexure stage that permits us to follow the crack tip as it advances through the different microstructural regions.

RESULTS

Figure 3 reveals the matrix orientation between two fibers for a low HTT of 1100°C. The composite is unidirectional, with the fiber being mesophase-based E75 (modulus of 75Mpsi ≅ 520 GPa) from DuPont, and the matrix is PAA. The SAD pattern is consistent with the layer planes oriented parallel to the fibers, as expected based on the previous discussion and evidence from optical microscopy and SEM.[1,2] Note the rippling or striation effect in the matrix. These striations run perpendicular to the layer-plane orientations and are believed to be the result of the interaction of the ion beam with the oriented layer planes.[5] Following higher HTTs, the matrix reveals a highly lamellar texture, brought out by the ion milling (Figure 4); SADs of this region confirmed its highly graphitized nature.

One immediate consequence of this strain-induced, oriented, and graphitized matrix interphase in C/C is that the matrix becomes a two-phase system, the second phase being the nongraphitized, glassy carbon. We would expect, therefore, that the *average* density and shrinkage of a thermoset-resin-derived matrix will depend on the relative proportion of the two different carbon structures and their respective densities. Furthermore, we would expect the amount of graphitized interphase to increase with the fiber volume fraction (ignoring the complicating

2
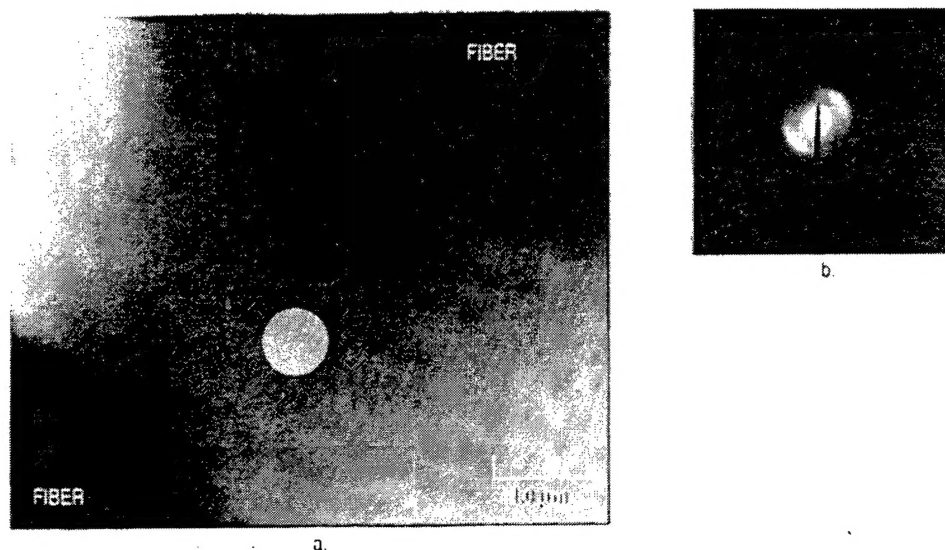
Figure 3. Transverse sections of carbonized unidirectional composites: (a) BF image of E75/PAA/1100°C; (b) matrix SAD of aperture zone in (a). (Reprinted from *Carbon* 32(1), G. S. Rellick and P. M. Adams, TEM Studies of Resin-Based Matrix Microstructure in Carbon/Carbon Composites," 127–44, Copyright 1994, with permission from Elsevier Sciences Ltd, Pergamon Imprint.)

2 μm

Figure 4. Kink bands in transverse section of T50/SC1008/2900°C, BF image. (Reprinted from *Carbon* 32(1), G. S. Rellick and P. M. Adams, TEM Studies of Resin-Based Matrix Microstructure in Carbon/Carbon Composites," 127–44, Copyright 1994, with permission from Elsevier Sciences Ltd, Pergamon Imprint.)

3

factor of fiber distribution). We recently attempted a measurement of the in situ matrix shrinkage and in situ density as a function of HTT for a series of unidirectionals fabricated fr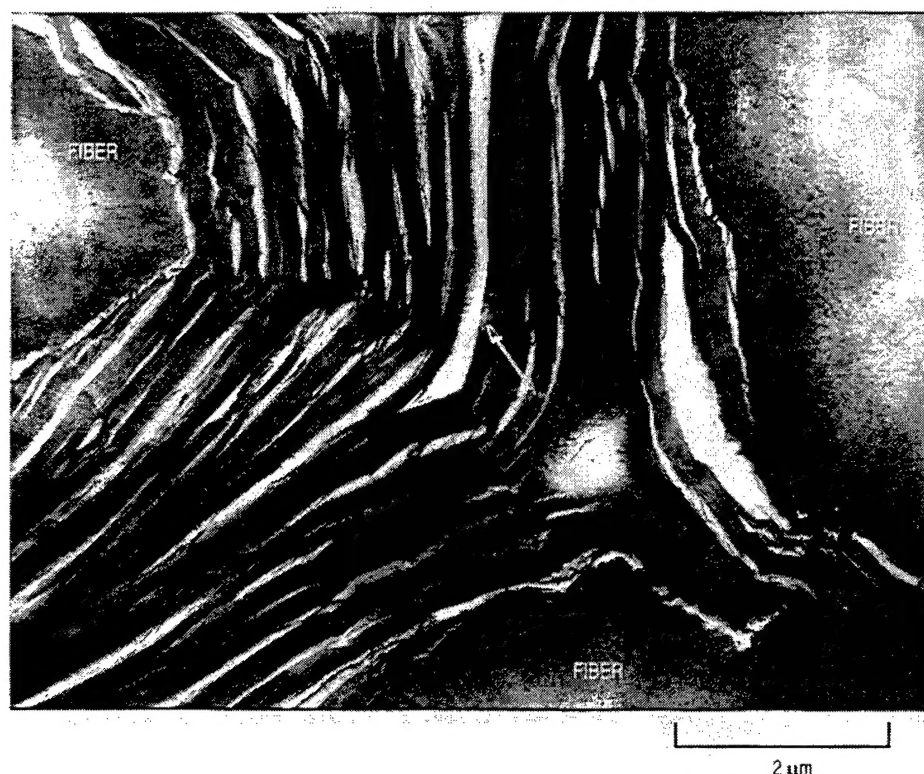om T50 fiber and both PAA resin and phenolic resin.[6] The results confirmed our suspicions—for both resin-matrix precursors, the average matrix density for each HTT from 1800 to 2750°C increased with fiber volume fraction. In addition, there were significant density differences between the two matrices. For example, the density of the phenolic-derived matrix after 2750°C HTT was 1.90 g/cm^3, while for the PAA-derived matrix, it was only 1.77 g/cm^3. The respective fiber volume fractions were 0.45 and 0.32.

It was a characteristic feature of the phenolic resin to consolidate more efficiently and, thereby, yield a higher fiber volume composite. However, the higher density may also have had a contribution from a greater "intrinsic" graphitizability of the phenolic resin. It was not possible to separate this effect from the fiber-volume effect. However, to repeat, both matrices showed a positive dependence of density on fiber volume fraction, thereby establishing this as a real effect.

A much more interesting, but certainly more complicated, issue is the role of the matrix (and the interphase region) in C/C fracture behavior. We recently studied this phenomenon by using an in situ SEM flexure stage in order to observe the interactions between the advancing crack tip and the microstructural features of the composite in the frontal process zone. The composite was a single-tow unidirectional made with DuPont E130 fiber and PAA-resin precursor. A sketch of the experiment is shown in Figure 5.

A number of interesting phenomena were observed for HTTs of 1100 to 2400°C. Following the lowest HTT of 1100°C, failure was dominated by the well-bonded brittle matrix; a tortuous crack path in the E130 fibers (Figure 6) appeared to contribute to a relatively high utilization of fiber strength in spite of this brittle matrix
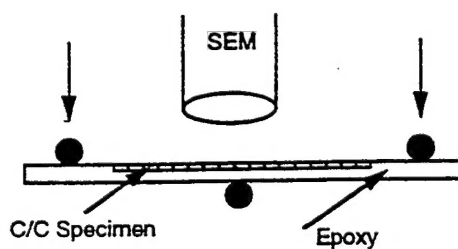

Figure 5. Schematic diagram of experimental arrangement for in situ flexure testing
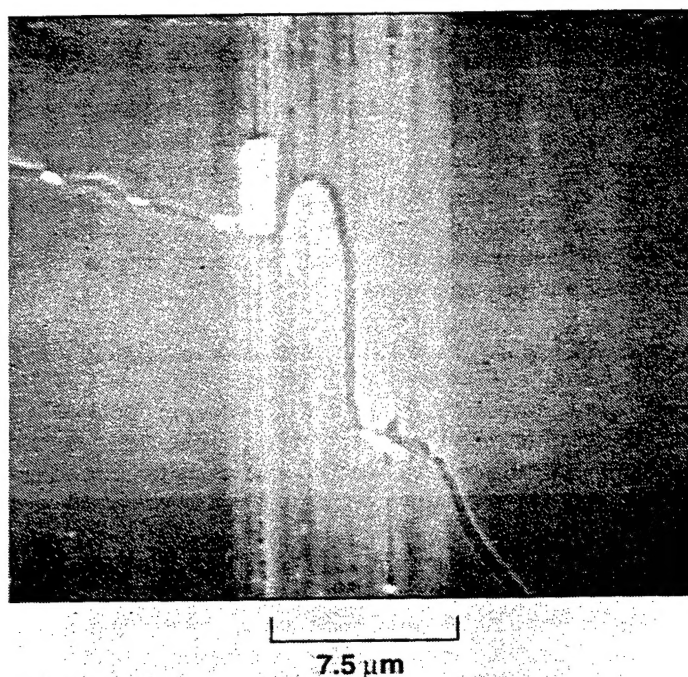
4

7.5 μm

Figure 6. View of crack propagation in E130 composite prior
to crack opening revealing intrafilament crack deflection.

failure. We attempted to calculate the interfacial shear stress (IFSS) that might be
generated by matrix shrinkage during pyrolysis of the polymer to carbon. These
values were compared to approximate calculations of crack-tip interfacial shear
stresses using the Cook-Gordon approach. The results suggested that the strong
bonding in the 1100°C HTT composite and the consequent absence of crack
deflection cannot be accounted for by friction alone, and, therefore, chemical
bonding or some type of fiber-matrix mechanical interlocking must be involved.

Higher HTTs lead to progressive weakening of the fiber-matrix interface, thereby
reducing the likelihood of matrix-dominated failure. For a HTT of 1600°C, we
observe fiber bridging across matrix cracks; this bridging contributes to crack-tip
shielding by the filaments. However, there are still well-bonded regions that
result in brittle crack propagation. The result typically is a mixed-mode type of
failure. With heat treatment to 2150°C, multiple matrix cracking (MMC) is
observed. Using the crack-spacing model of Aveston, Cooper, and Kelly (ACK),
an IFSS of 6 MPa was estimated for the MMC case. Attempts to calculate the
matrix failure strain using the ACK formulation led to a large overprediction of
the failure strain, although a number of the parameters used in the calculation are
known only very approximately. In addition, the onset of matrix interphase
(sheath) structure development is also first evident at the 2150°C HTT. In Figure
7 the interphase microstructure for the 2150°C HTT is seen in the SEM photo to
cause blunting of the crack, but no deflection of the crack along the sheath
(interphase) length. Something approaching an optimum strength utilization is
realized from the 2150°C HTT, based on independent uniaxial tensile tests.[8] As
discussed previously,[2] this interphase is a region of higher preferred orientation
and enhanced crystalline development[5] as a consequence of matrix deformation
during pyrolysis and carbonization. For the case of the SEM in Figure 7, the
greater brightness of the sheath is most likely the result of its higher density,[6]
which results in a higher electron emission. Also, because of the relatively low
HTT of 2150°C, this matrix interphase sheath structure is not highly graphitized
and, therefore, in contrast, does not have the lamellar graphitic texture seen in the
highly graphitized E130 fiber adjacent to it.

5

With heat-treatment to 2400°C, the oriented matrix interphase now becomes well graphitized, as evidenced by its lamellar texture, and is almost indistinguishable from the graphitic E130 fiber (Figure 8 compared to Figure 7). Crack blunting at

Figure 7. High-magnification micrograph showing crack blunting in interfacial region of 2150°C heat-treated composite.
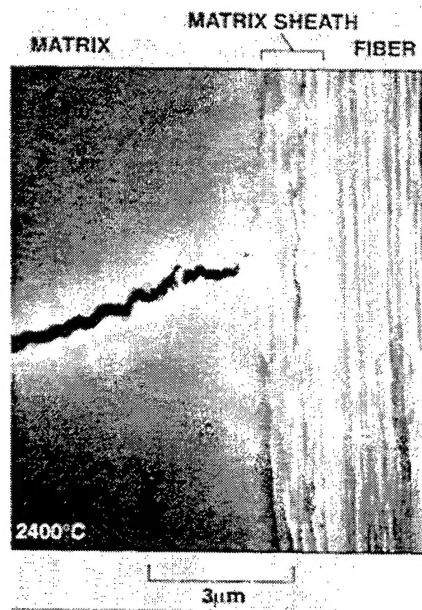

Figure 8. High-magnification micrograph showing crack blunting at graphitized matrix sheath structure in 2400°C heat-treated composite.

6

the graphitized matrix sheath is also shown in Figure 8. The high degree of orientation and lamellar graphitic structure of the sheath leads to significant delamination cracking in the sheath along the direction of the filament (Figure 9). However, this intramatrix cohesive failure also reduces the load-carrying capabilities of the matrix. Figure 10 is a higher-magnification view of a crack zone showing well-defined regions of nongraphitized matrix, graphitized matrix sheath, and fiber. Note the extensive debonding between fiber and matrix.

Following the highest HTT of 2750°C, the development of the graphitized sheath interphase is very extensive along the length of the interfacial region. Figure 11 shows a sequence of two micrographs of the composite as it is strained. As the crack propagates across the width of the composite, it is first deflected around a zone of sheath (left side of Figure 11a). The fiber associated with this sheath has been removed by polishing. The crack then becomes blunted at fiber F after it passes through a second sheath. Further straining (Figure 11) leads to partial fracture of filament F and extensive longitudinal splitting of the matrix sheath region labeled S. Note the saw-toothed structure of the fractured sheath. At this point, the intra-matrix cohesive failure of the sheath is very extensive, leading to a decoupling of the surrounding matrix from the fibers. In addition to the very weak coupling between fiber and matrix for this HTT, in a previous study, we also found evidence of fiber degradation resulting from the C/C processing.[8]

Figure 9. Short-range longitudinal intramatrix splitting in 2400°C heat-treated composite.

Figure 10. Crack zone showing well-defined regions of non graphitized matrix, graphitized sheath, and fiber in 2400°C heat-treated composite.

CONCLUSIONS

Carbon/Carbon composites that are produced with a thermosetting-resin matrix precursor form a distinct interphase of graphitized matrix adjacent to the fibers. This interphase "sheath" can be as large as 1–2 μm in thickness. This structure differs significantly from carbon matrix, which is at the same distance from the fiber and which does not experience the orienting stresses at the interface, which are believed responsible for the development of the stress-oriented and graphitizable structure. Rather, this matrix, although usually fairly well oriented, remains glassy, i.e., nongraphitic in structure. In many ways, it resembles the structure of PAN-based carbon fibers. The structure of this interphase can be studied most effectively by SEM and TEM. The development of a graphitized-carbon interphase can have major effects on properties. Two are discussed in this publication. The first is the effect on matrix density and associated matrix shrinkage. The other is the effect on mechanical properties. The latter is much more complicated and involves phenomena such as crack-tip blunting in the interphase in the early stages of its development and longer-range crack deflection as well as intramatrix cohesive failure in the later stages of development (HTTs of 2400 and 2750°C) where the interphase becomes highly graphitized.
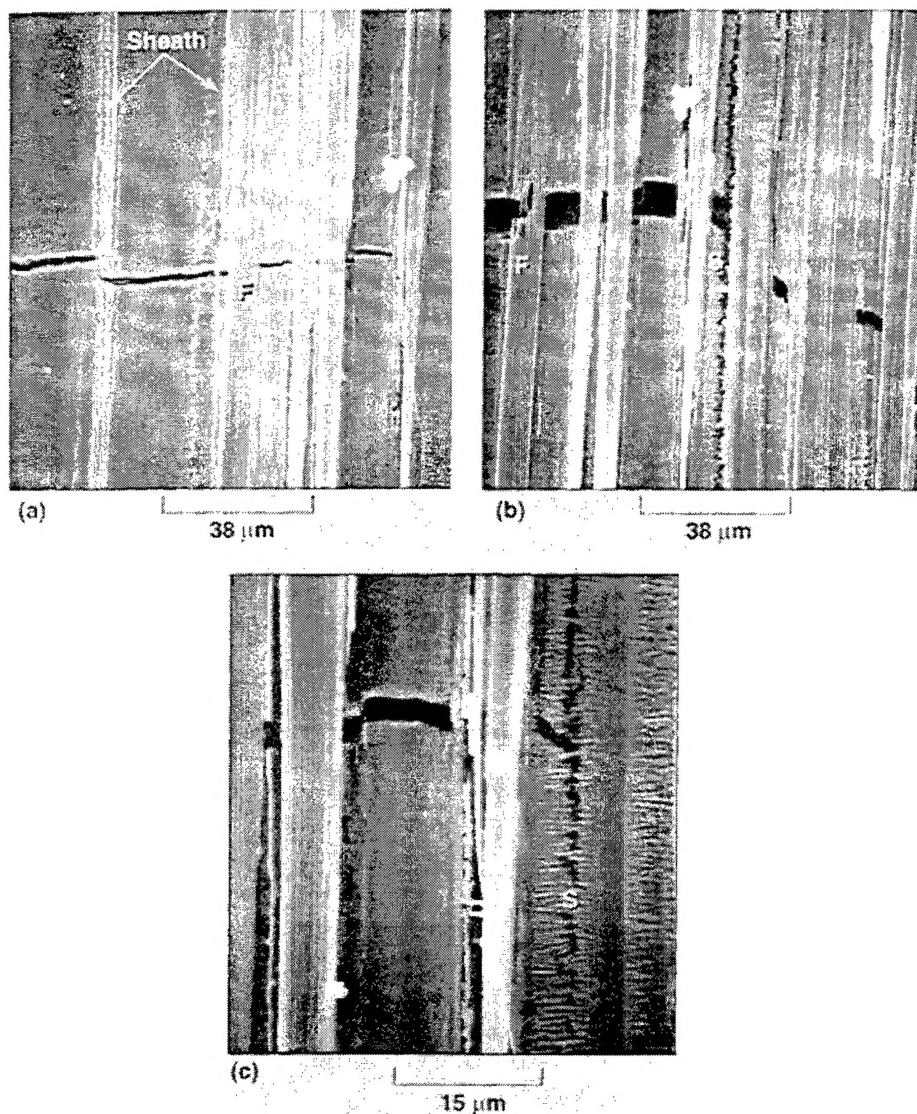
8

Figure 11. Crack propagation through a 2750°C heat-treated composite at two different degrees of strain.

REFERENCES

1. R. J. Zaldivar and G. S. Rellick, "Some Observations on Stress Graphitization in Carbon-Carbon Composites," *Carbon 29*, 1155–1163 (1991).

2. G. S. Rellick, D. J. Chang, and R. J. Zaldivar, "Mechanisms of Orientation and Graphitization of Hard-Carbon Matrices in Carbon/Carbon Composites," *J. Materials Research 7*, 2798–2809 (1992).

3. R. J. Zaldivar, G. S. Rellick, and J. M. Yang, "Processing Effects on the Mechanical Behavior of Polyarylacetylene-Derived Carbon-Carbon Composites," *SAMPE J. 27*, 29–36 (Sept/Oct 1991).

4. R. J. Zaldivar, R. W. Kobayashi, G. S. Rellick, and J. M. Yang, "Carborane-Catalyzed Graphitization in Polyarylacetylene-Derived Carbon-Carbon Composites," *Carbon 29*, 1145–1153 (1991).

5. G. S. Rellick and P. M. Adams, "TEM Studies of Resin-Based Matrix Microstructure in Carbon/Carbon Composites," *Carbon* 32(1), 127–44 (1994).

6. G. S. Rellick and R. J. Zaldivar, "In Situ Matrix Properties in Unidirectional Carbon/Carbon Composites," *Ext. Abst., 21st Biennial Conf. on Carbon*, Buffalo, New York, pp. 68–69 (1993).

7. R. J. Zaldivar, G. S. Rellick, and J. M. Yang, "Failure Modes of the Unidirectional Ultra-High Modulus Carbon-Fiber/Carbon-Matrix Composite," *J. Amer. Ceram. Soc.*, submitted for publication.

8. R. J. Zaldivar, G. S. Rellick, and J. M. Yang, "Fiber Strength Utilization in Carbon-Carbon Composites," *J. Materials Research*, 8(3), 501–511 (1993).

TECHNOLOGY OPERATIONS

The Aerospace Corporation functions as an "architect-engineer" for national security programs, specializing in advanced military space systems. The Corporation's Technology Operations supports the effective and timely development and operation of national security systems through scientific research and the application of advanced technology. Vital to the success of the Corporation is the technical staff's wide-ranging expertise and its ability to stay abreast of new technological developments and program support issues associated with rapidly evolving space systems. Contributing capabilities are provided by these individual Technology Centers:

Electronics Technology Center: Microelectronics, VLSI reliability, failure analysis, solid-state device physics, compound semiconductors, radiation effects, infrared and CCD detector devices, Micro-Electro-Mechanical Systems (MEMS), and data storage and display technologies; lasers and electro-optics, solid state laser design, micro-optics, optical communications, and fiber optic sensors; atomic frequency standards, applied laser spectroscopy, laser chemistry, atmospheric propagation and beam control, LIDAR/LADAR remote sensing; solar cell and array testing and evaluation, battery electrochemistry, battery testing and evaluation.

Mechanics and Materials Technology Center: Evaluation and characterization of new materials: metals, alloys, ceramics, polymers and composites; development and analysis of advanced materials processing and deposition techniques; nondestructive evaluation, component failure analysis and reliability; fracture mechanics and stress corrosion; analysis and evaluation of materials at cryogenic and elevated temperatures; launch vehicle fluid mechanics, heat transfer and flight dynamics; aerothermodynamics; chemical and electric propulsion; environmental chemistry; combustion processes; spacecraft structural mechanics, space environment effects on materials, hardening and vulnerability assessment; contamination, thermal and structural control; lubrication and surface phenomena; microengineering technology and microinstrument development.

Space and Environment Technology Center: Magnetospheric, auroral and cosmic ray physics, wave-particle interactions, magnetospheric plasma waves; atmospheric and ionospheric physics, density and composition of the upper atmosphere, remote sensing, hyperspectral imagery; solar physics, infrared astronomy, infrared signature analysis; effects of solar activity, magnetic storms and nuclear explosions on the earth's atmosphere, ionosphere and magnetosphere; effects of electromagnetic and particulate radiations on space systems; component testing, space instrumentation; environmental monitoring, trace detection; atmospheric chemical reactions, atmospheric optics, light scattering, state-specific chemical reactions and radiative signatures of missile plumes, and sensor out-of-field-of-view rejection.